Title	Regional Anatomical Observation of Morphology of Greater Palatine Canal and Surrounding Structures
Author(s)	Suzuki, M; Omine, Y; Shimoo, Y; Yamamoto, M; Kaketa, A; Kasahara, M; Serikawa, M; Rhee, S; Matsubayashi, T; Matsunaga, S; Abe, S
Journal	Bulletin of Tokyo Dental College, 57(4): 223-231
URL	http://hdl.handle.net/10130/5827
Right	
Description	

Bull Tokyo Dent Coll (2016) 57(4): 223–231

Original Article

doi:10.2209/tdcpublication.2016-1100

Regional Anatomical Observation of Morphology of Greater Palatine Canal and Surrounding Structures

Masashi Suzuki[1,2], Yuya Omine[1], Yoshiaki Shimoo[1,3], Masahito Yamamoto[1], Akihiro Kaketa[4], Masaaki Kasahara[1], Masamitu Serikawa[1], Sunki Rhee[1], Tadatoshi Matsubayashi[1], Satoru Matsunaga[1] and Shinichi Abe[1]

[1] *Department of Anatomy, Tokyo Dental College, 2-9-18 Misaki-cho, Chiyoda-ku, Tokyo 101-0061, Japan*
[2] *Ginza Yanagidouri Dental Clinic, 1-5-11 Ginza, Chuo-ku, Tokyo 104-0061, Japan*
[3] *Malo Clinic Tokyo, 7-8-10 Ginza, Chuo-ku, Tokyo 104-0061, Japan*
[4] *Kaketa Dental Office, 1-2-16 Aoba-ku, Sendai 980-0014, Japan*

Received 10 February, 2016/Accepted for publication 21 April, 2016

Abstract

In maxillary molar region implant therapy, support is sometimes obtained from trabecular bone comprising the maxillary tuberosity, pterygoid process of the sphenoid bone, and pyramidal process of the palatine bone. Great care is necessary in such cases due to the presence of the greater palatine canal, which forms a passageway for the greater palatine artery, vein, and nerve. However, clinical anatomical reports envisioning embedding of pterygomaxillary implants in this trabecular bone region have been limited in number. In this study, the 3-D morphology of the greater palatine canal region, including the maxillary tuberosity region and points requiring particular care in pterygomaxillary implantation, were therefore investigated. Micro-CT was used to image 20 dentulous jaws (40 sides) harvested from the dry skulls of Japanese individuals with a mean age of 28.2 years at time of death. The skulls were obtained from the Jikei University School of Medicine cadaver repository. Three-dimensional reconstruction of the trabecular bone region, including the greater palatine canal, was performed using software for 3-D measurement of trabecular bone structure. Trabecular bone region morphometry was performed with the hamular notch-incisive papilla (HIP) plane as the reference plane. The results showed a truncated-cone structure with the greater palatine foramen as the base extending to the pterygopalatine fossa. This indicates the need for care with respect to proximity of the dental implant body to the greater palatine canal and the risk of perforation if it is embedded in the maxillary tuberosity region at an inclination of 60° toward the lingual side. Moreover, caution must be exercised to avoid possible damage to the medial wall of the maxillary sinus if the inclination of the embedded dental implant body is almost perpendicular to the HIP plane.

Key words: Greater palatine canal — Dental implant — Maxillary tuberosity — Morphology — Skull

Introduction

Performing implantation in the maxillary molar region is generally considered difficult[1,12,17], partly due to the small operative field and presence of the maxillary sinus[14]. A number of procedures have been developed to resolve these difficulties, including bone generation, sinus lift, and zygomatic and pterygomaxillary implants[12,17]. Pterygomaxillary implants are usually embedded in the maxillary tuberosity or pterygoid process of the sphenoid bone. This is because there is only minimal change in trabecular bone structure in these areas over time, which means they offer an optimal locus for implant therapy. There have been several reports on pterygomaxillary implants. Khayat and Nader[10] noted a pterygomaxillary implant survival rate of 88.2% in edentulous patients of a mean age of 60 years, and Candel *et al.*[2] noted a mean take rate of 90.7% for implants embedded in the maxillary tuberosity region, together with a high level of post-prosthesis patient satisfaction.

Many researchers have examined the regional anatomy of the maxillary tuberosity and pterygoid process of the sphenoid bone together with their surroundings. In such studies, the locus comprising the maxillary tuberosity, pterygoid process of the sphenoid bone, and pyramidal process of the palatine bone is usually referred to as the trabecular bone region. It has been noted that trabecular bone structure is resistant to change under tractive force originating in the surrounding masticatory and palatine muscles over time[18]. The greater palatine canal is an important constituent in this region. It forms the passageway for the greater palatine artery, vein, and nerve, and serves as an important landmark in dental anesthesiology[8]. In this light, many researchers have investigated the locus of the greater palatine foramen as the outlet of the greater palatine canal[3,11,13,14], and reconstruction of the anatomical morphology of the greater palatine canal and the pterygopalatine fossa from 3-D structure images obtained by cone-beam CT has also recently been reported[9]. Little has been reported, however, on the clinical anatomy of the trabecular bone region with respect to the embedding of pterygomaxillary implants. The purpose of the present study was to investigate the 3-D morphology of the greater palatine canal, including the maxillary tuberosity region, and discuss its implications for pterygomaxillary implantation.

Materials and Methods

A total of 20 Japanese human skulls were used in this study. All the skulls were obtained from individuals aged between 15 and 44 years at time of death (mean age, 28.2 years). All were obtained from the cadaver repository of the Jikei University School of Medicine. All were from individuals with healthy teeth and jaws with no abnormal osseous damage or deformity or dental damage. They were selected based on bilateral absence of maxillary wisdom tooth eruption and clear presentation of the maxillary tuberosity.

The materials were imaged using a micro-CT system (HMX-225Actis4; Tesco Co., Tokyo, Japan) under the following basic conditions: tube voltage, 100 kV; tube current, 70 μA; strength, $\times$2.5; slice width, 50 μm; matrix size, 512$\times$512; slice voxel size, 140$\times$140$\times$50 μm; and imaging intensifier, 4-inch. The raw data consisted of 1,200 images obtained with a CCD camera with 16 bits per inch and 1,024$\times$1,024 scan lines; reverse projection was used for the 2-D slice data.

1. Observation of osseous morphology in 3-D reconstruction

Three-dimensional reconstructions were obtained from the slice images using 3-D reconstruction software (Tri-3D/BON, RATOC, Tokyo, Japan) for observation of osseous morphology in the trabecular bone region.

2. Osseous morphometry

Osseous morphometric analysis of the 3-D reconstructions was performed with the same

Fig. 1 Hamular notch-incisive papilla (HIP) plane taken as virtual plane of occlusion

∗: greater palatine canal.

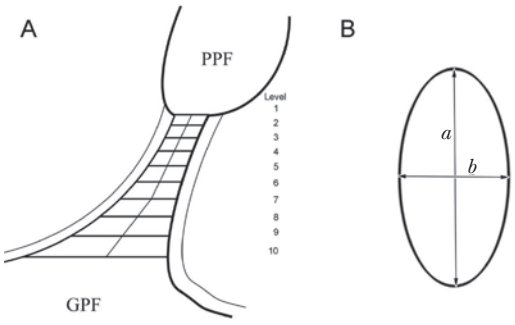

Fig. 2 Greater palatine canal morphometry

Panel A: 10 levels in height of greater palatine canal as measured from HIP plane. Panel B: greater palatine canal length (anteroposterior diameter) denoted as *a* and width denoted as *b*. PPF: pterygopalatine fossa; GPF: greater palatine foramen.

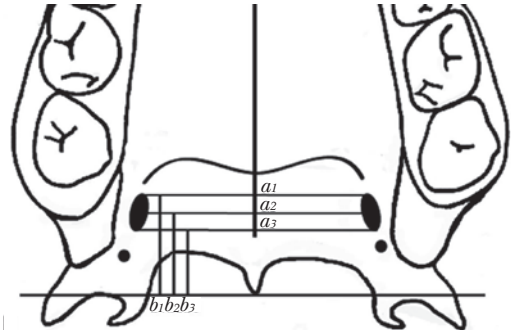

Fig. 3 Morphometry of greater palatine foramen and surrounding structures

Line segments connecting greater palatine canals bilaterally denoted as a_1, a_2, and a_3; perpendiculars from those segments to corresponding posterior nasal spine denoted as b_1, b_2, and b_3.

software (Tri-3D/BON). The hamular notch-incisive papilla (HIP) plane, which is generally regarded as the virtual occlusal plane[4], was taken as the reference plane as defined above. The measurement points were on the hard tissue at the posterior extremity of the incisive fossa and the lowest point on the left-right pterygomaxillary suture (Fig. 1). Such tissue is believed to undergo only minimal change over time, especially in dentulous jaws[7].

In measuring the greater palatine canal, the length was defined as the distance from the lowest point of the pterygopalatine fossa to the corresponding region of the greater palatine foramen, with its height in each specimen measured in terms of 10 levels starting from the HIP plane of the greater palatine canal (Fig. 2A), and its anteroposterior length and its width denoted as *a* and *b*, respectively (Fig. 2B). Anteroposterior length and width were compared using a *t*-test, with the level of significance set at 5% ($p<0.05$).

In observing and measuring the greater

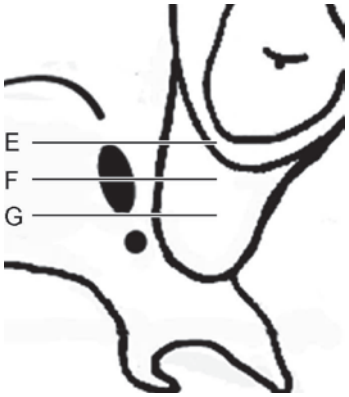

Fig. 4 Reference plane for measurements of greater palatine canal and its surrounding structures in frontal section, with canal divided into two by E, F, and G

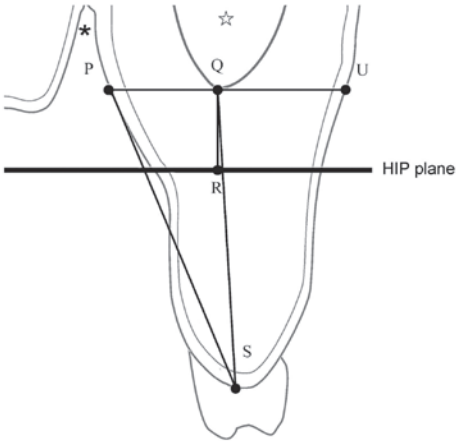

Fig. 5 Morphometry of greater palatine canal and surrounding structures in frontal section

P: intersection of line parallel to HIP plane at lowest point of maxillary sinus and greater palatine canal medial wall; Q: lowest point of maxillary sinus; R: point where line passing through Q crosses HIP plane perpendicularly; S: alveolar crest; U: intersection of line parallel to HIP plane at lowest point of maxillary sinus and lateral wall of alveolar region.
∗: greater palatine canal, ☆: Maxillary sinus.

palatine foramen from the palatine side, three lines between the left and right greater palatine foramina marked the anterior, medial, and posterior regions of the greater palatine foramen, and were denoted as a_1, a_2, and a_3, respectively (Fig. 3); the lengths of the perpendiculars b_1, b_2, and b_3 (Fig. 3) drawn from each of these lines, respectively, to the corresponding posterior nasal spine region were measured.

In measuring distances between the greater palatine foramen and the surrounding structures, a section including the third molar at fixed points E, F, and G (Fig. 4) was obtained, and, on this plane, points P, Q, R, S, and U were designated (Fig. 5). The measured distances comprised the horizontal distance between the outer side of the greater palatine canal and the medial wall of the maxillary sinus (P–Q); the perpendicular distance between the maxillary sinus medial wall and the HIP plane (Q–R); and the linear distance between the outer side of the greater palatine canal and the maxillary tuberosity (P–S). The measured angles ∠SPU and ∠SQU were those formed by points P, Q, R, S, and U (Fig. 5) on planes perpendicular to the HIP plane and passing through points E, F and G.

All measurements were performed by the same examiner at intervals of 1 week to reduce intra-examiner error.

Results

1. Analysis of trabecular bone region in 3-D reconstruction

The morphology of the greater palatine canal resembled a truncated cone, with the bottom of the pterygopalatine fossa as its top and the palatine region as its base (Fig. 1). The greater palatine canal approached the medial wall of the maxillary sinus (Fig. 6B) and extended to the maxillary palatine process and greater palatine foramen. The lesser palatine foramen extended posteriorly and opened to the posterior region of the palatine bone plate (data not shown). The interior region of the maxillary tuberosity presented a structure of sparse cancellous bone covered with cortical bone (Fig. 6C). The pterygomaxillary suture was located posterior to the maxillary sinus (Fig. 6A).

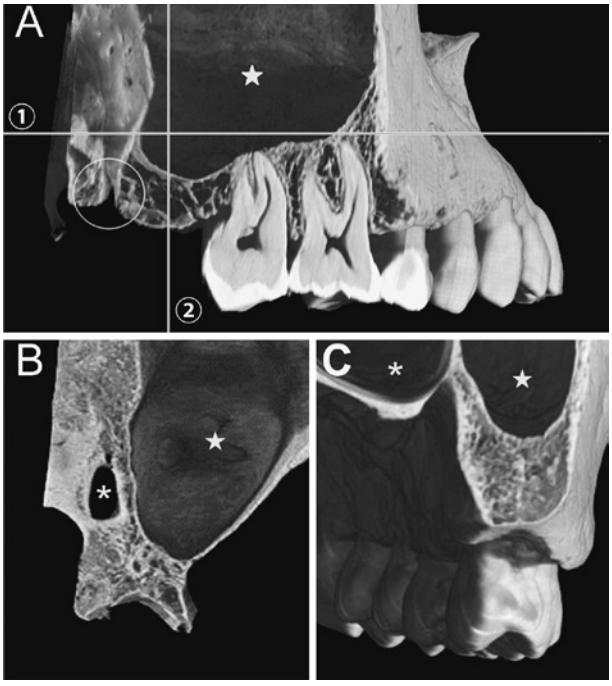

Fig. 6 Images of greater palatine canal and surrounding structures

Panel A shows external aspect of pterygomaxillary suture (circled) and maxillary sinus (☆), with Lines ① and ② indicating position of horizontal and sagittal sections shown in Panels B and C. Panel B shows cranial aspect (view from above) of greater palatine canal (*) and maxillary sinus (☆) in horizontal section. Panel C shows dorsal aspect (view from posterior) of greater palatine canal (*) and maxillary sinus (☆) in frontal section.

2. Osseous morphometry

The greater palatine canal presented a morphology resembling a truncated cone, with a cross-section that tended to be generally larger in the anteroposterior direction at the medial wall of the maxillary sinus; this tendency increased with growing proximity to the palate. The measured values tended to be largest in the region near the palate (the base), with both the anteroposterior length and width decreasing as the measurement proceeded upwards, but again increasing in the region near the pterygopalatine fossa (the top). The anteroposterior length and width of the greater palatine canal were thus both largest at Level 10 and smallest at Level 4 (Table 1); the length was significantly larger than the width at all of Levels 1–10 (Table 2). In summary, the results showed that the greater palatine canal presents an elliptical cross-section extending from the pterygopalatine fossa region (the top) to the palatal region (the base), with a greater diameter in the anteroposterior direction.

Observation and measurement of the greater palatine foramen from the palatine side showed distance b_1 to be larger than b_2 or b_3, and a_1 to be larger than a_2 or a_3, with no substantial difference between b_2 and b_3 or between a_2 and a_3 (Table 3).

Measurement of the distances between the greater palatine foramen and the surrounding structures showed no differences between planes E, F, and G in distance P–Q; they also

Table 1 Length and width of the greater palatine canal

Level	Length	Width
	Mean (mm)	Mean (mm)
1	2.81	2.01
2	2.58	1.91
3	2.57	1.86
4	2.53	1.78
5	2.61	1.86
6	2.71	1.97
7	2.96	2.31
8	3.08	2.2
9	3.51	2.41
10	3.96	2.72

Table 2 Summary of Student's *t*-test for comparing length and width of the greater palatine canal

Level	L and W	p-value
1	*	$p<0.001$
2	*	$p<0.01$
3	*	$p<0.001$
4	*	$p<0.001$
5	*	$p<0.001$
6	*	$p<0.001$
7	*	$p<0.001$
8	*	$p<0.001$
9	*	$p<0.001$
10	*	$p<0.001$

Statistically significant differences: $p<0.05$

showed uniform spacing of the alveolar bone between the greater palatine canal and maxillary sinus. Distance P–S was found to be larger than distances P–Q or Q–R (Table 4). The mean values of the measured angles on the planes perpendicular to the HIP plane and passing through points E, F and G were 49.8° for ∠SPU and 82.1° for ∠SQU (Table 5).

Table 3 Linear measurements between the greater palatine canal and surrounding structures (1)

Measurement	Mean (mm)	SD
a_1	33.60	3.3
a_2	29.80	1.1
a_3	30.10	2.1
b_1	10.20	6.8
b_2	9.20	3.2
b_3	9.10	2.2

SD: standard deviation

Discussion

Chrcanovic and Custódio[3] reported that the greater palatine foramen was 14 mm distal to the median palatine suture; that it was located on the opposite side of the third molar in 54.87% of skulls, distal to the third molar in 38.94%, and between the maxillary second and third molars in 6.19%; and that in many skulls it opened in the anteromedial direction. Slavkin[15] also reported that the greater palatine foramen was found 1–3 mm distal to the third molar in adult bones. In the present study, the designation of three points (E, F, and G) on the greater palatine foramen was investigated as a means of identifying aspects requiring particular care in greater palatine canal implant therapy. The results indicate that the risk of damaging the greater palatine canal in implant therapy can be accurately assessed on this basis, despite such physical differences in the location of the greater palatine foramen.

It is generally recognized that the direction of opening on the greater palatine canal axis in the lateral aspect is approximately 50–60°, and that the angle with the greater palatine canal anterior wall diminishes sharply below the medial region, strongly tending to become more acute than that of the long axis. It has also been reported that the structure of the greater palatine canal widens toward the base, thus resembling the shape of a folding fan[5].

Table 4 Linear measurements between the greater palatine canal and surrounding structures (2)

	P–Q		Q–R		P–S	
	Mean (mm)	SD	Mean (mm)	SD	Mean (mm)	SD
E	8.1	6.4	7.7	6.4	14.4	6.4
F	7.1	3.1	7.1	3.1	14.1	8.1
G	8.2	4.2	8.2	4.2	13.2	4.2

SD: standard deviation

Table 5 Measured angles of the greater palatine canal and surrounding structures

∠ SPU		∠ SQU	
Mean (°)	SD	Mean (°)	SD
49.8	12.1	82.1	9.3

SD: standard deviation

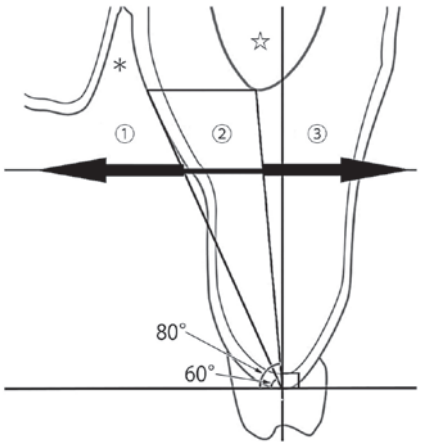

Fig. 7 Risk classification scheme for implant embedding showing greater palatine canal (*) and maxillary sinus (☆)

① Most Vulnerable Zone; ② Vulnerable Zone; ③ Least Vulnerable Zone. Left hand side (right hand side) arrow indicates ① Most Vulnerable Zone (③ Least Vulnerable Zone).

The present results support this finding. This clearly indicates that the opening in the greater palatine foramen is large, which raises concern about the risk of excessive palatal inclination in implant embedding.

Hongo *et al.*[7] reported that the pterygomaxillary suture, which serves as the posterior reference in the HIP plane, is located in the region of the connection between the maxillary tuberosity of the maxillary bone posterior surface and the region of entry of the pyramidal process of the palatine bone to the alisphenoid notch. It is generally recognized that the pterygomaxillary suture is obscured in an edentulous jaw, but it can be clearly recognized in a dentulous jaw. The incisive canal opening region in the incisive fossa region resists change over time, even with tooth loss. In the present study, the standard deviation of the measured angles of the greater palatine canal and surrounding structures showed less variation. This suggests that measuring the greater palatine canal in dentulous jaws with the HIP plane determined on hard tissue could be highly useful in performing implant therapy.

In implant surgery in the maxillary tuberosity region, the risks of palatal perforation, nerve damage, and maxillary sinus posterior perforation are among the matters of primary concern. With a pterygomaxillary or other relatively long implant, in particular, it is essential to exercise care in regard to its proximity to the greater palatine canal and nerve[2,16]. The largest value found for ∠SPU in the present study was approximately 60°, which clearly raises concern in regard to proximity to the greater palatine canal and risk of perforation in embedding an implant in the

maxillary tuberosity region with a palatal inclination of 60°. It was therefore concluded that the following 3 areas represented decreasing order of risk of perforation on the palatal side: the Most Vulnerable Zone, in which the implant angle toward the palatal side is 60° or less; the Vulnerable Zone, in which it is 60–80°; and the Least Vulnerable Zone, in which it is 80° or more (Fig. 7). At the same time, it was also determined that the risk of damage to the maxillary sinus medial wall increases in the Vulnerable Zone, in which the inclination angle of implant embedding more closely approaches the perpendicular to the HIP plane. In the Least Vulnerable Zone, finally, it was concluded that the risk of damage to the greater palatine canal may be regarded as vanishingly small, but care is essential in regard to proximity of the implant body to the maxillary sinus.

In pterygoid plate implantation, it is generally recommended that a relatively long implant (20 mm) be implanted with an inclination of 45° in the sagittal plane[6], but little has been reported in regard to basic measurement of the distance from the alveolar ridge region to the greater palatine canal. In regard to linear measurements between the greater palatine canal and maxillary tuberosity (distance P–S), the present results showed that the mean distance was between 13.2 and 14.4 mm (Table 4). This indicates that an implant with the recommended length of 20 mm and a palatal inclination will tend to preclude maintenance of an effective distance between the greater palatine canal and alveolar crest region, and thus may result in close proximity to the canal.

Acknowledgement

The authors are deeply grateful to the teachers at the Department of Anatomy at Tokyo Dental College for their guidance and proofreading in the completion of this manuscript and to all at the Tokyo Dental College Oral Health Science Center for their assistance in the performance of the measurements.

References

1) Balshi TJ, Lee HY, Hernandez RE (1995) The use of pterygomaxillary implants in the partially edentulous patient: a preliminary report. Int J Oral Maxillofac Implants 10:89–98.
2) Candel E, Peñarrocha D, Peñarrocha M (2012) Rehabilitation of the atrophic posterior maxilla with pterygoid implants: a review. J Oral Implantol 38:461–466.
3) Chrcanovic BR, Custódio AL (2010) Anatomical variation in the position of the greater palatine foramen. J Oral Sci 52: 109–113.
4) Cooperman HN (1975) HIP plane of occlusion in oral diagnosis. Dental Surv 51:60–62.
5) Douglas R, Wormald PJ (2006) Pterygopalatine fossa infiltration through the greater palatine foramen: where to bend the needle. Laryngoscope 116:1255–1257.
6) Graves S (1994) The pterygoid plate implant: a solution for restoring the posterior maxilla. Int J Periodontics Restorative Dent 14: 513–523.
7) Hongo T, Kato T, Kase K (1986) Anatomical research on the H.I.P. plane of Japanese. Shikwa Gakuho 86:1563–1571. (in Japanese)
8) Howard-Swirzinski K, Edwards PC, Saini TS, Norton NS (2010) Length and geometric patterns of the greater palatine canal observed in cone beam computed tomography. Int J Dent doi:10.1155/2010/292753
9) Hwang SH, Seo JH, Joo YH, Kim BG, Cho JH, Kang JM (2011) An anatomic study using three-dimensional reconstruction for pterygopalatine fossa infiltration *via* the greater palatine canal. Clin Anat 24:576–582.
10) Khayat P, Nader N (1994) The use of osseointegrated implants in the maxillary tuberosity. Pract Periodontics Aesthet Dent 6:53-61.
11) Methathrathip D, Apinhasmit W, Chompoopong S, Lertsirithong A, Ariyawatkul T, Sangvichien S (2005) Anatomy of greater palatine foramen and canal and pterygopalatine fossa in Thais: considerations for maxillary nerve block. Surg Radiol Anat 27: 511–516.
12) Peñarrocha M, Carrillo C, Boronat A, Peñarrocha M (2009) Retrospective study of 68 implants placed in the pterygomaxillary region using drills and osteotomes. Int J Oral Maxillofac Implants 24:720–726.
13) Piagkou M, Xanthos T, Anagnostopoulou S, Demesticha T, Kotsiomitis E, Piagkos G, Protogerou V, Lappas D, Skandalakis P, Johnson EO (2012) Anatomical variation and morphology in the position of the palatine foramina in adult human skulls from Greece.

J Craniomaxillofac Surg 40:e206–e210.
14) Saralaya V, Nayak SR (2007) The relative position of the greater palatine foramen in dry Indian skulls. Singapore Med J 48:1143–1146.
15) Slavkin HC (1965) Anatomical investigation of the greater palatine foramen and canal. Alpha Omegan 58:148-151.
16) Tulasne JF (1992) Osseointegrated fixtures in the pterygoid region, Advanced Osseointegration Surgery: Applications in the Maxillofacial Region, Worthington P, Branemark PI (Eds), pp.182–188, Quintessence, Chicago.
17) Valerón JF, Valerón PF (2007) Long-term results in placement of screw-type implants in the pterygomaxillary-pyramidal region. Int J Oral Maxillofac Implants 22:195–200.
18) Yamaura T, Tamatsu Y, Ide Y (1998) Study on figure and internal structure of maxillary tuberosity in Japanese. Nihon Kōkū Inpuranto Gakkai Shi 11:23–42. (in Japanese)

Correspondence:
Dr. Masahito Yamamoto
Department of Anatomy,
Tokyo Dental College,
2-9-18 Misaki-cho, Chiyoda-ku,
Tokyo 101-0061, Japan
E-mail: yamamotomasahito@tdc.ac.jp